Journal of Colloid and Interface Science 455 (2015) 110–116

Contents lists available at ScienceDirect

Journal of Colloid and Interface Science

www.elsevier.com/locate/jcis

The new aspects of the anticorrosive ZnO@SiO_2 core–shell NPs in stabilizing of the electrolytic Ni bath and the Ni coating structure; electrochemical behavior of the resulting nano-composite coatings

Zahra Sharifalhoseini [a,*], Mohammad H. Entezari [a,b]

[a] Sonochemical Research Center, Department of Chemistry, Faculty of Science, Ferdowsi University of Mashhad, 91779 Mashhad, Iran
[b] Environmental Chemistry Research Center, Department of Chemistry, Faculty of Science, Ferdowsi University of Mashhad, 91779 Mashhad, Iran

GRAPHICAL ABSTRACT

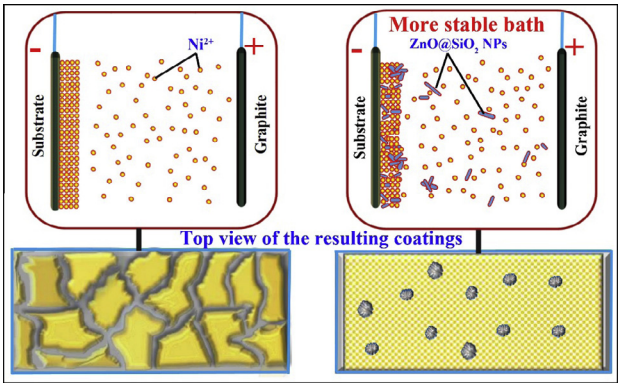

ARTICLE INFO

Article history:
Received 5 May 2015
Accepted 21 May 2015
Available online 29 May 2015

Keywords:
ZnO@SiO_2 NPs
Stability enhancement
Nano-composite deposit

ABSTRACT

The pure phase of the ZnO nanoparticles (NPs) as anticorrosive pigments was synthesized by the sonication method. The surfaces of the sono-synthesized nanoparticles were covered with the protective silica layer. The durability of the coated and uncoated ZnO NPs in the used electrolytic Ni bath was determined by flame atomic absorption spectrometry. In the present research the multicomponent Ni bath as the complex medium was replaced by the simple one. The used nickel-plating bath was just composed of the Ni salts (as the sources of the Ni^{2+} ions) to better clarify the influence of the presence of the ZnO@SiO_2 core–shell NPs on the stability of the medium. The effect of ZnO@SiO_2 NPs incorporation on the morphology of the solid electroformed Ni deposit was studied by scanning electron microscopy (SEM). Furthermore, the influence of the co-deposited particles in the Ni matrix on the corrosion resistance of the Ni coating was evaluated by the electrochemical methods including linear polarization resistance (LPR) and Tafel extrapolation.

1. Introduction

Due to the importance of the corrosion protection of the metallic and even nonmetallic constructions, effective strategies have been developed to reduce the high cost of corrosion worldwide.

* Corresponding author. Fax: +98 5138795457.
E-mail addresses: Z.sharifhoseini@yahoo.com (Z. Sharifalhoseini), entezari@ferdowsi.um.ac.ir (M.H. Entezari).

http://dx.doi.org/10.1016/j.jcis.2015.05.047
0021-9797/

Among different preventive strategies, coating technology as an important scientific field has attracted a wide range of the researches. One of the practical importance of the coating is the creation of the barrier layer between the substrate and its environmental medium to protect or reduce the corrosion rate [1].

Over the years, other technologies have been developed in this field to improve the coating structures. In the past decades, nanotechnology has been extensively used in the various fields of the science such as medicine, biology, chemistry, materials science, and engineering. The use of the nano-sized materials in the coating technology due to unique properties and higher efficiency than bulk materials has attracted so much attention of researchers [2,3].

Ni electroplating as an electrochemical important process has been used for deposition of the nickel layer, which is applied to control the corrosion as the natural and harmful phenomenon [4]. Scientific reports have claimed that adding some micro- and nano-sized particles such as Al_2O_3 [5,6], SiC [7], ZrO_2 [8,9], TiO_2 [10,11], $SrSO_4$ [12], Si_3N_4 [13] SiO_2 [14], WC [15], B_4C [16] and diamond nanoparticles [17] suspended in the electroless and electroplating baths results in the co-deposition of these particles along with the pure metal or alloy deposition. Incorporation of the micro- and nano-sized particles by the formation of the micro- and nano-composite electroformed-solid phase enhances the strength of the resulting metal film.

Among the inorganic materials used for co-deposition, zinc oxide (ZnO) has been less attended to fabricate the nano-composite coating, whereas many methods are available for the large-scale synthesis of this low-cost, nontoxic, and anticorrosive inorganic material [18–20]. Despite the fact that zinc oxide has high stability in the harsh temperature and pressure applied in the industrial processes, shows poor stability in the acid and basic baths.

In this research, the ZnO NPs have been chosen as anticorrosive agents for co-deposition in the Ni bath. In order to increase the stability of the particles, the surface of the ZnO NPs has been coated with the thin layer of SiO_2. As it is known, SiO_2 due to high chemical stability has been considered as an ideal shell to protect the inner core [21,22]. In these series of experiments, the bath composed of the several components has been replaced by the simple Ni bath to disclose the new aspect of the nanoparticles contribution in stabilizing of the Ni plating medium. In this paper, we show how the addition of the ZnO@SiO_2 NPs to the simple Ni bath in addition to the enhancement of the durability of the ZnO NPs particles could prevent the medium from decomposing. Indeed, the applying of this simple bath has been provided the conditions in which the role of the core–shell nanoparticles in stabilizing of the medium was clearer.

Furthermore, the effect of the incorporation of the coated ZnO NPs on the morphology of the electroformed Ni structure and its corrosion inhibition performance has been studied. With the help of the electrochemical measurements and concerning the amount of the embedded ZnO and ZnO@SiO_2 NPs in the Ni matrix, the influence of the SiO_2 shell on improvement in the corrosion resistance of the final coating has been determined.

2. Experimental

2.1. Materials

Zinc chloride, potassium hydroxide (used for the ZnO NPs synthesis), absolute ethanol, TEOS (>98%), and concentrated ammonia solution (25%) (used for the ZnO NPs coating), and nickel sulfate, nickel chloride and sodium chloride (used for the Ni electroplating) were purchased from Merck company and used without purification. The mild steel (composed of Fe – 99.340, Cu – 0.043, Sn – 0.001, Co – 0.007, Al – 0.059, Ni – 0.031, Mo – 0.001, Ti – 0.001, P – 0.013, S – 0.033, Cr – 0.028, C – 0.024, Si – 0.058, Mn – 0.387-wt.%) was chosen as substrate.

2.2. Procedure

2.2.1. Activation of the substrate and preparation of the bath

The steel substrate was cut into the specimens with dimensions of 20 mm × 20 mm × 1 mm. To remove oil and grease from the surface, the substrate was cleaned by the acetone. To have the smooth surface for uniform electroplating each sample was polished by an abrasive paper. The passive oxide layer of the metal was removed by immersing the plate into a beaker containing of hydrochloric acid (12 M HCl) for 30 s. After rinsing with distilled water and the neutralization of excess acid by NaOH aqueous (1 M), the surface of each sample was activated by soaking the plate in acid solution (HCl, 0.1 M). The resulting surface due to high susceptibility to oxidation should be placed in the plating bath immediately after treatment.

To have a reliable control of temperature during the reaction, Ni electroplating was carried out in the cell equipped with a water jacket.

In the present research, nickel sulfate and nickel chloride were used to provide the Ni^{2+} ions and the sodium chloride to enhance the electrical conduction. To find the influence of the incorporation of the ZnO@SiO_2 NPs on the bath stability, some other materials, which were generally used in the Ni bath such as complexing and buffering agents, were not added to this medium. The natural pH of the medium was about 5.5. To prevent the pH reduction, during the Ni electroplating the pH was adjusted within the range of 4.8–5.0 by the addition of a dilute NaOH solution.

The volume of the plating bath was 100 cc and the rectangular graphite with the dimensions 20 mm × 10 mm × 2 mm was used as the anode. Because of decomposition of this simple bath in the absence of the ZnO@SiO_2 NPs after about 30 min, and for having a meaningful comparison between the coating formed in the bath with and without nanoparticles, electroplating was lasted 30 min. The bath composition and operating conditions are summarized in Table 1.

2.2.2. Preparation of the ZnO@SiO_2 NPs

The ZnO@SiO_2 core–shell NPs were prepared in two steps, including the synthesis of the ZnO NPs and the coating of the resultant particles with a shell of SiO_2. The procedure used for the synthesis of the ZnO NPs was the same method applied in our previous work [23]. The procedure in summary as follows: under the ultrasonic irradiation, 50 ml of 0.5 M $ZnCl_2$ was added to 50 ml of 1 M KOH solution at 80 °C. The resulting white precipitates were collected, washed with distilled water, and dried at 80 °C for 18 h.

The coating process of the ZnO NPs surface was carried out according to the method reported for the fabrication of the core–shell magnetic nanomaterial [24]. In this method, 0.5 g ZnO NPs were dispersed in 35 ml distilled water. After adding 140 ml of

Table 1
The plating bath composition and the applied electrodeposition parameters.

Deposition parameters	Amount
Concentration of $NiSO_4$	5.00 (g/100 ml)
Concentration of $NiCl_2$	1.50 (g/100 ml)
Concentration of NaCl	0.50 (g/100 ml)
ZnO NPs, ZnO@SiO_2 NPs	0.025 (g/100 ml)
T	70.00 (°C)
Time	30.00 min
Current density	12.50 (mA/cm^2)
pH	4.80–5.00

absolute ethanol and 2.5 ml of ammonia solution (2.5%) to the ZnO NPs suspension, 2.04 ml of the tetraethyl orthosilicate (TEOS) was periodically added to the above solution (0.34 ml per hour). The coating process was performed under the constant stirring (600 rpm). The precipitates were collected and washed with distilled water several times. The resultant sample was put in an oven at 80 °C for 18 h.

2.3. Estimation of the embedded core–shell nanoparticles in the Ni matrix

The strategy applied to evaluate the amount value of the embedded core–shell nanoparticles in the coating as follows: the ZnO@SiO_2 NPs were collected carefully after Ni electroplating, washed with distilled water, and weighed. The difference between the initial and the final amount of the ZnO@SiO_2 NPs were considered as the sum of the incorporated particles into the Ni matrix and those particles, which probably were dissolved, in the electrolytic Ni bath.

To estimate the amount of the nanoparticles probably was dissolved during co-deposition, the residual solution of the Ni bath after centrifugation and complete separation of the nanoparticles was analyzed by using a flame atomic absorption spectrometer (Shimadzu, AA-670). As it is known, this technique is used for determining the concentration of a particular element in a sample. Therefore, applying this chemical analysis provided information about the content of the zinc element (zinc content was considered equivalent to the amount of Zn^{2+} ions). For this purpose, 2 ml of the residual solution of the bath (with final volume of 90 ml) was diluted 50 times and this sample was analyzed to determine the concentration of zinc element.

2.4. Evaluation of the corrosion resistance of the coatings

To provide the results with better accuracy, two different electrochemical methods were applied. The linear polarization resistance (LPR) method as a rapid and accurate technique was chosen to evaluate the polarization resistance of the coatings. LPR measurements were performed by the ACM instrument (Gill AC potentiostat) through a three-electrode cell, in which test sample was used as working electrode, the platinum wire served as counter electrode, and a saturated calomel electrode (SCE) used as the reference electrode. In this method after measurement of open circuit potential (E_{OCP}) and its stabilization, small perturbation of potential applies (10 mV below to 10 mV above of the E_{OCP} at low scan rate of 0.166 mV/s). Generally, the plot of the applied potential versus the measured current is linear in this small range of potential and its slope is named as polarization resistance (R_p) [25].

To evaluate the corrosion resistance of the species through the Tafel extrapolation, potentiodynamic polarization (PDP) measurements carried out by the potential scanning in the wide range of potential (200 mV in both the positive and negative directions from the open circuit potential at a scan rate of 1 mV/s). These electrochemical measurements were performed by using a potentiostat/galvanostat (SAMA 500; Electro-analysis System) through a conventional three electrode cell, including the bare surface (mild steel) and the coated surfaces as working electrode, platinum wire as counter electrode, and Ag/AgCl as the reference electrode. The measured current density in the logarithmic scale was plotted versus the applied potential.

Both LPR and potentiodynamic polarization measurements were performed in non-deaerated conditions at room temperature and before any scanning, the species were immersed in the corrosive medium (NaCl solution 3.5 wt.%) for 30 min to stabilize the open circuit potential (E_{OCP}). The exposed surface area of the test sample to the corrosive medium was 1 cm^2.

3. Results and discussion

3.1. Characterization of ZnO and ZnO@SiO_2 NPs

The crystallographic structure and the morphology of the sono-synthesized ZnO NPs showed that the pure phase of the zinc oxide were synthesized and the white resulting powders were crystallized in the nanorod structures (XRD analysis and the TEM images of the fabricated ZnO NPs are given in the Supplementary data). In the case of the ZnO@SiO_2 NPs, the FTIR analysis was performed and the presence of the typical vibration bands of SiO_2 including Si–O–Si symmetric stretching at 803 cm^{-1}, Si–O–Si asymmetric stretching at 1090 and 1170 cm^{-1}, and Si–O–H stretching vibration at 953 cm^{-1} confirmed that the surface of ZnO NPs was coated successfully with silica. (FTIR spectra of the coated and uncoated ZnO NPs are given in the Supplementary data.)

3.2. Characterization of electroformed Ni deposit and Ni/ZnO@SiO_2 nano-composite coating

3.2.1. SEM analysis

The surface morphology of the coatings was examined using a 3D microscope (LEO 1450 VP). Fig. 1 points to the SEM images of the electroformed Ni coating without core–shell NPs.

Fig. 1(a) and (b) show the surface of the Ni deposit at the magnifications of 1000× and 5000×. As it is seen, the entire surface is covered with many cracks. This feature was assigned to the oxidation of the Ni film due to the exposure to the air (SEM images were taken two weeks after electroplating) and confirmed that the resulting coating had no good quality. Indeed, the oxygen element detected by EDS analysis affirmed the oxidation of this weak Ni deposit, whereas incorporation of the ZnO@SiO_2 NPs in the Ni matrix led to form the different morphology. Fig. 2 displays the Ni deposit containing the core–shell NPs.

It is clear that the deposition of the core–shell ZnO@SiO_2 NPs improved the basic structure of the coating. The micro- and nano-size particles, which were embedded in the Ni matrix acted as a glue or cement to bind the electroformed phase structure together.

The effective collision between the particles and the metal surface resulted in trapping of these particles in the growing solid metal phase. These particles could act as the primary nuclei, accumulation of the other particles on the external surface of these primary nuclei and the simultaneous Ni electroplating could be formed larger particles.

Since the agglomeration of the nanoparticles did not observe on the coating surface formed in a complex electrolytic Ni bath (the results are not shown here), the formation of these large particles could be related to the ionic strength of the medium. The existence of more molecular forces, including attraction and repulsion between the different species in the complex medium (composed of more components) could decrease the possibility of the agglomeration of the particles. High magnification of one of these aggregates (Fig. 2(b)) shows that its surface was covered with the Ni film and some cracks on the surface could be observed. It seems that the negative effects associated with the presence of the cracks in these points are less than produced on the bulk coating. Because these shadow cracks on the surface of the agglomerated particles (Fig. 2(c)) exposes the ZnO@SiO_2 particles (with high corrosion resistance) to the corrosive medium, whereas the presence of the

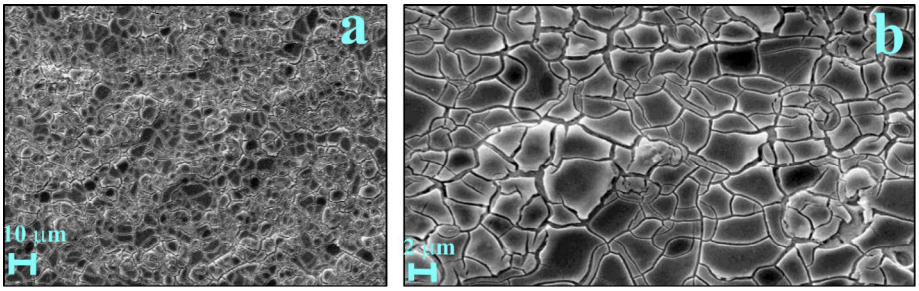

Fig. 1. SEM images of the Ni deposit; (a) and (b) are attributed to the Ni surface at different magnifications (1000× and 5000×), the existence of the cracks entire the surface is due to the oxidization of the weak Ni layer.

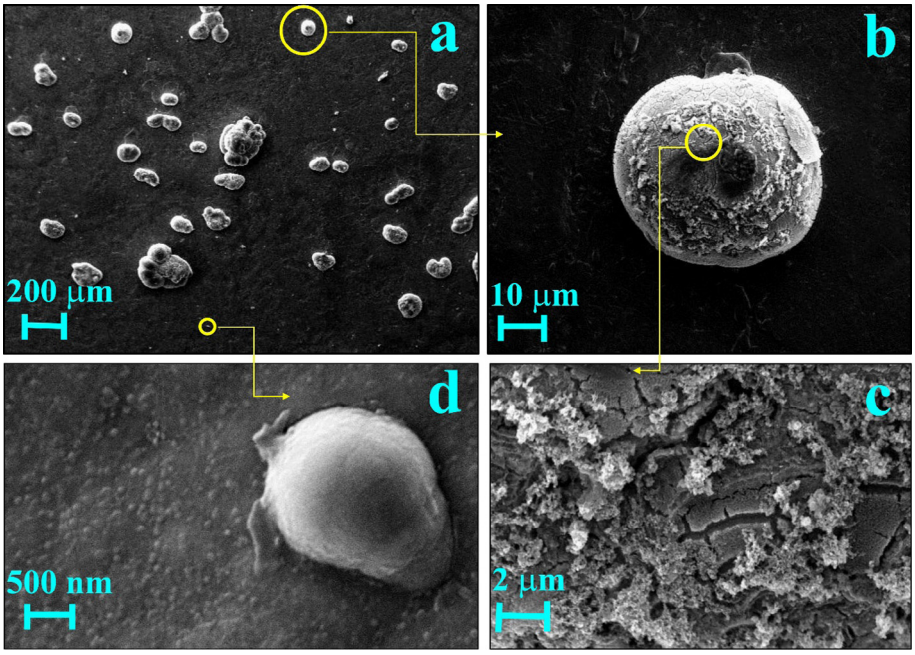

Fig. 2. SEM micrographs of the Ni/ZnO@SiO_2 nano-composite coating; (a) shows the surface of the coating at low magnification (the micro-size particles detected on the surface are due to the agglomeration of the particles), (b) points to one isolated micro-sized particle, (c) displays the cracks on the surface of the agglomerated area, and high magnification of the surface (d).

deep cracks in the Ni coating (Fig. 1) leads to the exposure of the bare surface of the mild steel (which is more prone to corrosion) to the corrosive medium.

Furthermore, observation of many small nubs with uniform distribution (Fig. 2(d)) could be attributed to the presences of the embedded ZnO@SiO_2 NPs in Ni deposit. Simultaneous Ni plating and the deposition of the particles led to the cover of the embedded particles with the gray thin film of the Ni.

3.2.2. EDS analysis

The EDS spectra and chemical composition of the Ni deposit with and without core–shell NPs were determined by energy dispersive X-ray analysis (EDX) coupled to SEM microscope and the results are shown in Fig. 3.

As it was mentioned, for the Ni deposit, the presence of the oxygen confirmed the oxidation of the surface due to the exposure to the air. The existence of iron is attributed to the detection of the sublayer of the Ni film (the presence of the cracked points exposed the mild steel consisted mostly of iron (99%) to the beam electron of the SEM instrument).

In the case of the second deposit, the chemical composition of the surface was reported for two different locations of the coating. One of them is attributed to the bulk, and another one is attributed to the agglomerated area. In both cases, the EDX analysis confirmed the presence of the expected elements, including zinc, oxygen, nickel, and silicon. The weight percent of the defined areas marked on Fig. 3 are given in the inserted tables (analysis on some other points showed about same trend).

3.3. Evaluation of the amount of the loaded core–shell nanoparticles in the Ni matrix

The absorbance value of Zn in the diluted solution determined by the flame atomic absorption spectrometry was 0.214. As it is known, this analytical method is not absolute and the calibration standard sample is required to measure other elements (calibration was based on the silver element, the absorbance value of 0.239 is equal to the 1 ppm of the silver concentration). Therefore, the concentration of the Zn element by considering the dilution factor and the calibration scale was evaluated 0.0040 g.

On the other hand, the mass of the ZnO@SiO_2 NPs, which were collected carefully after electroplating, was 0.013 g. With regard to difference in the value of the initial and the final nanoparticles (which was equal 0.012 g) and the amount of the dissolved coated particles during electroplating (which was estimated 0.0040 g)

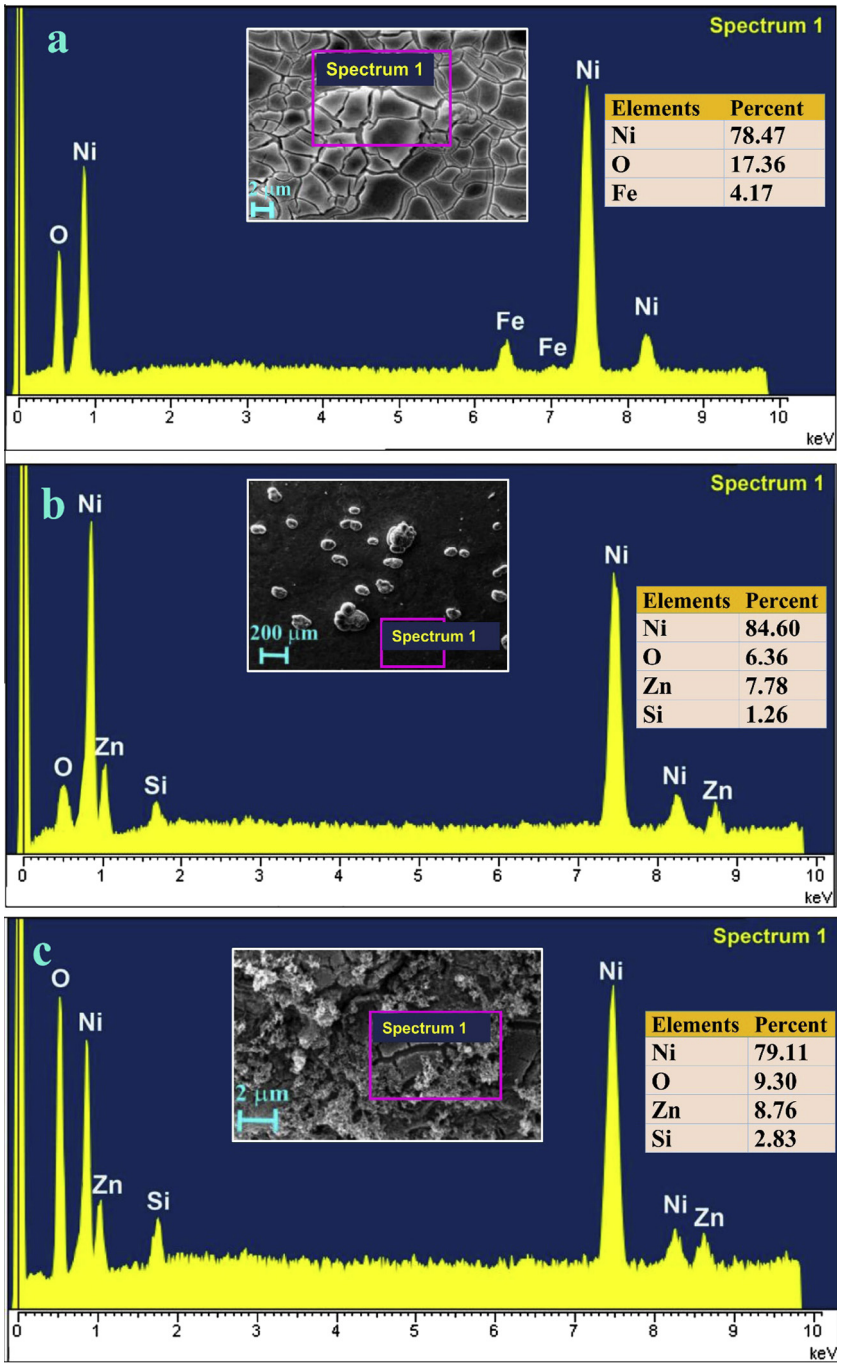

Fig. 3. EDS spectra and chemical composition of: (a) electroformed Ni deposit, (b and c) bulk and agglomerated area of the Ni/ZnO@SiO_2 nano-composite coating respectively. (The weight percent values are attributed to the defined area marked on each sample, measurements at other points showed almost the same trend.)

could be concluded that amount of the of embedded core–shell nanoparticles in the Ni matrix was about 0.0080 g. The absorbance value of Zn in the residual solution of the bath containing the ZnO NPs was 0.310 and the amount of the loaded ZnO NPs in the Ni matrix was estimated about 0.0058 g.

3.4. The influence of the presence of the nanoparticles on the bath conditions

Comparison of the plating through the Ni bath with and without nanoparticles showed that the presence of the coated and even uncoated ZnO NPs affected the stability of the medium. Our experiments showed that this simple Ni bath (despite the pH adjustment) started to decompose after about 30 min. As an interesting result, the addition of a small amount of nanoparticles (0.025 g) in this medium resulted in more stability of the bath even after 60 min. It seems that the nanoparticles, including ZnO@SiO_2 NPs and even the ZnO NPs by affecting the bath conditions control the progress of the reaction. To clarify the effect of these nanoparticles in pH changes, experiments were carried out without the addition of dilute NaOH solution. Therefore, the pH was not adjusted at the constant level during electroplating and its changes were monitored by the pH meter. The results showed that the reduction of this parameter in the absence of the coated and uncoated nanoparticles (ZnO and ZnO@SiO_2 NPs) was faster than their absence. Reduction in pH (from 5 to about 3.8) in the absence

of the nanoparticles was observed after about 6 min, whereas in the presence of the nanoparticles this reduction occurred after about 15 min. More stability of the medium and less reduction of pH value in the presence of the nanoparticles could be illustrated by the following reasons:

- The hydroxyl groups on the surface of the ZnO and ZnO@SiO_2 NPs (these groups exist on the surface of the most oxides [24]) could interact with the charged species in the medium. The electrostatic interactions between the oxygen of the hydroxyl groups with the Ni^{2+} ions control the free amount of the Ni^{2+} ions. Indeed the action of the nanoparticles in this state (which is shown graphically in Fig. 4(a)) was the same role of a complexing agent. The major function of the complexing agents is to stabilize the system by control of the cation release in the reaction medium.
- Progress of the reaction follows by the pH reduction. The affinity of the produced H^+ with the hydroxyl groups and the formation of the hydrogen bond (which is represented in the graphical view in Fig. 4(b)) could retard the sharp drop in the pH value.
- As it is known the rate of the Ni electroplating depends on the Ni^{2+} ion migration from the solution to the cathode surface and the concentration gradient of the ions results in the movement of the these ions from bulk to the surface. It seems that the presence of the suspended nanoparticles in the medium by the restriction of the ion diffusion could decrease the reaction rate. This phenomenon (which is shown graphically in Fig. 3(c)) could be proposed for the less pH reduction.

3.5. Effect of particle loading on the corrosion resistance

The electrochemical measurements were performed by the LPR technique and the values of the polarization resistance (R_p) were obtained for all samples. The values of the corrosion current were evaluated by the Stern–Geary equation, which defines a relationship between the corrosion current and the R_p:

$$i_{corr} = \left[\frac{\beta_a\beta_c}{2.303(\beta_a+\beta_c)}\right]\left[\frac{1}{R_p}\right]$$

in where, β_a and β_c are the anodic and cathodic Tafel slopes (V/dec) and R_p is the polarization resistance ($\Omega\ cm^2$) [26]. The electrochemical parameters for all specimens are summarized in Table 2.

Fig. 5 displays the Tafel plots of the bare surface, Ni coating, Ni/ZnO, and Ni/ZnO@SiO_2 nano-composite coatings.

The electrochemical data derived from Tafel curves, including the anodic and cathodic Tafel slops (β_a, β_c), corrosion current (i_{corr}), and corrosion potential (E_{corr}) are listed in Table 3.

The electrochemical measurements performed by LPR and Tafel extrapolation indicated that in both cases, the nano-composite coatings acquired slightly more noble character than the pure Ni film. Furthermore, more positive shift in the potential and the smaller current density for the Ni deposit containing core–shell particles implies that the Ni/ZnO@SiO_2 nano-composite coating is less prone to corrosion in comparison with the Ni/ZnO nano-composite coating. This higher inhibitory performance could be illustrated by the amount of the embedded nanoparticles in the metal matrix. The amount of the coated and uncoated ZnO NPs in the structure of the Ni deposit were estimated 0.0080 and 0.0058 g respectively (this ratio is about 1.4). It should be noted that if the amount of the embedded ZnO and ZnO@SiO_2 NPs were assumed equal, the Ni/ZnO@SiO_2 coating was still showing slightly more noble character than the Ni/ZnO deposit (the R_p ratios of Ni/ZnO@SiO_2 to the Ni/ZnO obtained from LPR and Tafel extrapolation are about 1.63 and 1.7 respectively). Therefore, in addition to the amount of the loaded nanoparticles, the nature of the compound affected the corrosion protection performance of the final

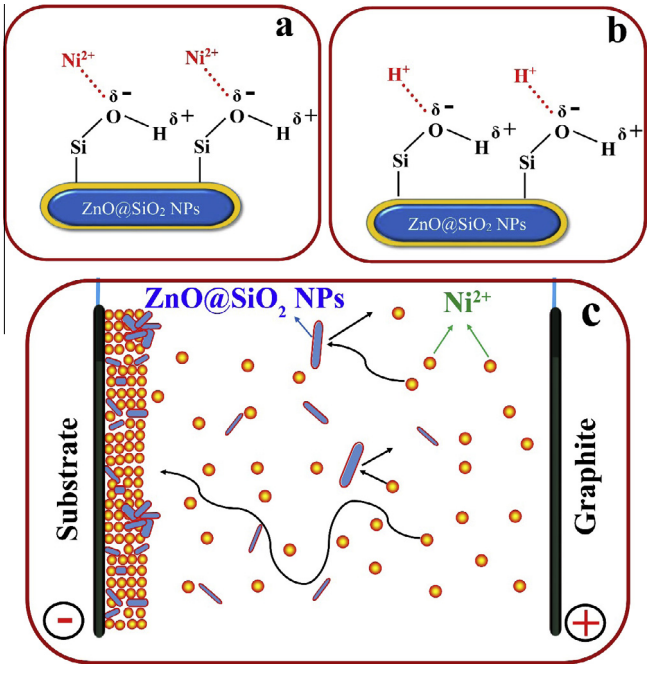

Fig. 4. The schematic view of the possible phenomena happen during co-deposition; (a) is attributed to the attaching of the Ni^{2+} ions to the hydroxyl groups on the ZnO@SiO_2 NPs, (b) affinity of the H^+ ions to the hydroxyl groups and the formation of the hydrogen bond, (c) restriction of the Ni^{2+} ion diffusion to the cathode surface. All proposed phenomena can affect the plating reaction, more stability of the medium and less reduction of pH value.

Table 2
Polarization resistance values of the samples obtained from LPR technique and the corrosion current values calculated from Stern–Geary equation.

Coating	E_{OCP}[a] (V vs. SCE)	B[b] (mV/dec)	R (kΩ cm^2)	i_{corr} (μA/cm^2)
Bare surface	−0.760	25.43	1.35	18.83
Ni	−0.402	21.29	5.34	3.98
Ni/ZnO	−0.311	54.83	17.35	3.16
Ni/ZnO@SiO_2	−0.299	31.27	28.45	1.08

[a] E_{OCP} values were reported after stabilization of the potential (E_{OCP} is often considered as E_{corr}).
[b] B values were calculated by Tafel slopes obtained from Tafel curves $\left(B=\frac{\beta_a|\beta_c|}{2.303(\beta_a+|\beta_c|)}\right)$.

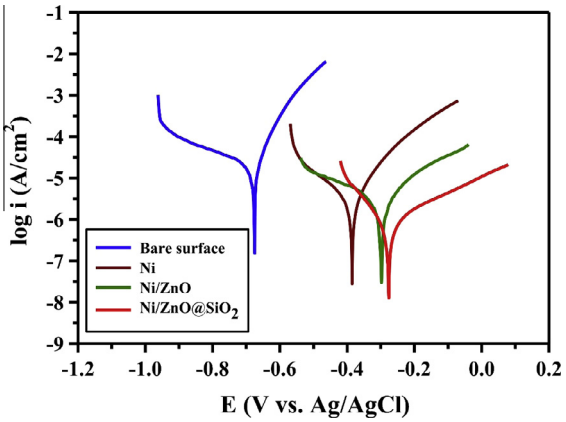

Fig. 5. Tafel plots of the samples.

Table 3
Electrochemical parameters of the samples derived from Tafel plots in 3.5 wt.% NaCl.

Coating	E_{corr} (V vs. Ag/AgCl)	β_a (mV/dec)	β_c (mV/dec)	R (kΩ cm^2)	i_{corr} (μA/cm^2)
Bare surface	−0.687	71	−335	1.44	17.65
Ni	−0.388	113	−152	4.86	4.38
Ni/ZnO	−0.302	230	−280	15.98	3.43
Ni/ZnO@SiO_2	−0.277	245	−102	27.32	1.14

coating. On the other word silica due to higher chemical stability gave the nano-composite coating with higher corrosion resistance.

In spite of the fact that the polarization resistance of the samples showed no too high values (even in the case of the nano-composite coatings, and it was due to the selection of the simple bath), applying of this Ni bath was better to reach a conclusion on the role of the nanoparticles in stabilizing of the medium.

4. Conclusion

The ZnO nanoparticles, which were synthesized by the sonication method as low cost, safe, nontoxic, and anticorrosive agent were as the core particles and the silica compound due to the high thermal and chemical stability was chosen as the shell to protect the inner core from dissolution in the Ni bath. The influence of the creation of the protective silica shell on the stability of the ZnO NPs in the Ni bath was evaluated by the flame atomic absorption spectrometry. The effect of the presence of the coated and uncoated ZnO NPs in the simple Ni bath was studied and the results showed that the addition of these nanoparticles prevents the Ni bath from decomposing. Additionally, the study of the pH changes of the medium indicated that these particles could retard the sharp drop in pH. The corrosion study of the samples confirmed that the incorporation of the silica-coated particles in the Ni deposit due to higher chemical stability gave the nano-composite coating with higher corrosion resistance. Based on the experimental results the more stability and the less pH reduction of the medium in the presence of the nanoparticles were illustrated.

Acknowledgments

The support of Ferdowsi University of Mashhad (Research and Technology) for this work (code 3/21049, date 08/03/2012) is appreciated. We would like to thank Dr. Moayed and Mr. Taji from Metallurgical and Materials Engineering Department of Ferdowsi University of Mashhad for helpful assistance in the corrosion studies.

Appendix A. Supplementary material

Supplementary data associated with this article can be found, in the online version, at http://dx.doi.org/10.1016/j.jcis.2015.05.047.

References

[1] D. Prasai, J.C. Tuberquia, R.R. Harl, G.K. Jennings, K.I. Bolotin, ACS Nano 6 (2012) 1102–1108.
[2] I. Perelshtein, G. Applerot, N. Perkas, E. Wehrschetz-Sigl, A. Hasmann, G.M. Guebitz, A. Gedanken, Appl. Mater. Interfaces 1 (2009) 361–366.
[3] J.N. Balaraju, V. Ezhil Selvi, V.K. William Grips, K.S. Rajam, Electrochim. Acta 52 (2006) 1064–1074.
[4] N. Kanani, Electroplating: Basic Principles, Processes and Practice, Elsevier Advanced Technology, Oxford, UK, 2004.
[5] A.C. Ciubotariu, L. Benea, M. Lakatos-Varsanyi, V. Dragan, Electrochim. Acta 53 (2008) 4557–4563.
[6] K.H. Hou, Y.C. Chen, Appl. Surf. Sci. 257 (2011) 6340–6346.
[7] M.R. Vaezi, S.K. Sadrnezhaad, L. Nikzad, Colloid Surf. A 315 (2008) 176–182.
[8] X. Shu, Y. Wang, C. Liu, A. Aljaafari, W. Gao, Surf. Coat. Technol. 261 (2015) 161–166.
[9] P. Makkar, D.D. Mishra, R.C. Agarwala, V. Agarwala, Ceram. Int. 40 (2014) 12013–12021.
[10] V. Niksefat, M. Ghorbani, J. Alloys Compd. 633 (2015) 127–136.
[11] P. Makkar, R.C. Agarwala, V. Agarwala, Adv. Powder Technol. 25 (2014) 1653–1660.
[12] X.S. Liang, J.H. Ouyang, Y.F. Li, Y.M. Wang, Appl. Surf. Sci. 255 (2009) 4316–4321.
[13] M. Srivastava, V.K. William Grips, K.S. Rajam, Mater. Lett. 62 (2008) 3487–3489.
[14] M. Islam, M. Rizwan Azhar, N. Fredj, T.D. Burleigh, O.R. Oloyede, A.A. Almajid, S. Ismat Shah, Surf. Coat. Technol. 261 (2015) 141–148.
[15] M. Stroumbouli, P. Gyftou, E.A. Pavlatou, N. Spyrellis, Surf. Coat. Technol. 195 (2005) 325–332.
[16] M. Ebrahimian-Hosseinabadi, K. Azari-Dorcheh, S.M. Moonir Vaghefi, Wear 260 (2006) 123–127.
[17] H. Zhou, N. Du, L. Zhu, J. Shang, Z. Qian, X. Shen, Electrochim. Acta 151 (2015) 157–167.
[18] S. Ma, R. Li, C. Lv, W. Xu, X. Goua, J. Hazard. Mater. 192 (2011) 730–740.
[19] H. Lu, F. Zheng, M. Zhang, M. Guo, Electrochim. Acta 132 (2014) 370–376.
[20] S. Dhoke, A. Khanna, T. Jai Mangal Sinha, Prog. Org. Coat. 64 (2009) 371–382.
[21] J. Wang, S. Zheng, Y. Shao, J. Liu, Z. Xu, D. Zhu, J. Colloid Interface Sci. 349 (2010) 293–299.
[22] S. Abramson, W. Safraou, B. Malezieux, V. Dupuis, S. Borensztajn, E. Briot, A. Bée, J. Colloid Interface Sci. 364 (2011) 324–332.
[23] Z. Sharifalhoseini, M.H. Entezari, R. Jalal, Surf. Coat. Technol. 266 (2015) 160–166.
[24] S. Hozhabr Araghi, M.H. Entezari, Appl. Surf. Sci. 333 (2015) 68–77.
[25] E. Rakanta, T. Zafeiropoulou, G. Batis, Constr. Build. Mater. 44 (2013) 507–513.
[26] A. Małecki, A. Micek-Ilnicka, Surf. Coat. Technol. 123 (2000) 72–77.